Corneal Biomechanical Properties from Two-Dimensional Corneal Flap Extensiometry: Application to UV-Riboflavin Cross-Linking

Sabine Kling,[1,2] *Harilaos Ginis,*[2] *and Susana Marcos*[1]

Purpose. Corneal biomechanical properties are usually measured by strip extensiometry or inflation methods. We developed a two-dimensional (2D) flap extensiometry technique, combining the advantages of both methods, and applied it to measure the effect of UV-Riboflavin cross-linking (CXL).

Methods. Corneal flaps (13 pig/8 rabbit) from the de-epithelialized anterior stroma (96 μm) were mounted on a custom chamber, consisting of a BK7 lens, a reflective retina, and two reservoirs (filled with Riboflavin and silicone oil). Stretching the corneal flap during five pressure increase/decrease cycles (0–30 mm Hg) changed the refractive power of the system, whose Zernike aberrations were monitored with a ray-tracing aberrometer. Porcine flaps were used to test the system. Rabbits were treated with CXL unilaterally in vivo following standard clinical procedures. Flaps were measured 1 month postoperatively. An analytical model allowed estimating Young's modulus from the change in surface (strain) and pressure (stress). Confocal microscopy examination was performed before, and at different times after CXL.

Results. Flap curvature changed with increased function of IOP in pig flaps (23.4×10^{-3} D/mm Hg). In rabbit flaps curvature changed significantly less in 1 month post CXL ($P = 0.026$) than in untreated corneas [17.0 vs. 6.36 millidiopter (mD)/mm Hg]. Young's modulus was 2.29 megapascals (MPa) in porcine corneas, 1.98 MPa in untreated rabbit corneas, and 4.83 MPa in 1 month post CXL rabbit corneas. At the same time, highly reflective structures were observed in the rabbit midstroma after treatment.

Conclusions. 2D flap extensiometry allows estimating corneal elasticity in vitro. The measurements are spatially resolved in depth, minimize the effects of corneal hydration, and preserve the integrity of the cornea. The method proved the efficacy of CXL in increasing corneal rigidity after 1 month in rabbits. (*Invest Ophthalmol Vis Sci.* 2012;53:5010–5015) DOI: 10.1167/iovs.12-9583

From the [1]Instituto de Óptica "Daza de Valdés," Consejo Superior de Investigaciones Científicas, Madrid, Spain; and the [2]Institute of Vision and Optics, University of Crete, Heraklion, Greece.

Supported by European Young Investigator Award Grant EURYI 05-102-ES, the Spanish Government Grants FIS2008-02065 and FIS2011-25637 (SM), and a Formación de Personal Investigador (FPI) Predoctoral Fellowship (SK).

Submitted for publication January 27, 2012; revised April 24, May 22, and June 19, 2012; accepted June 19, 2012.

Disclosure: **S. Kling**, None; **H. Ginis**, None; **S. Marcos**, None

Corresponding author: Sabine Kling, Instituto de Óptica "Daza de Valdés," Calle de Serrano 121, 28006 Madrid, Spain; sabine@io.cfmac.csic.es.

Understanding corneal biomechanical properties is critical to model the biomechanical response of pathological corneal tissue (i.e., keratoconus, a progressive corneal disease that debilitates corneal tissue), and to increase the predictability of surgical outcomes or treatments (i.e., intrastromal ring segments, corneal cross-linking, or incisional surgery). Various methods have been used in the past to estimate the corneal modulus of elasticity (Young's modulus). The most widespread applied method is strip extensiometry,[1–4] followed by corneal button inflation,[5,6] and whole globe inflation.[4–10] In these techniques, a load is applied (typically along one axis in strip extensiometry, or radially by increasing IOP in inflation techniques). The strain upon the applied stress is measured from the lateral elongation, axial apex displacement,[4] shift of mercury droplets attached on the corneal surface,[5,7] or from changes in the corneal radius of curvature.[10,11] A new technique to estimate the corneal biomechanical properties, by measuring the corneal deformation upon air puff applanation, has recently been suggested.[12,13] In all in vitro biomechanical measurements, corneal hydration plays a role as it affects the tissue's mechanical response.[14] Also different medical solutions alter the corneal hydration and, thus, the biomechanical properties of the tissue[15] (Kling S, et al. *IOVS* 2010;51:ARVO E-Abstract 4628). UV-riboflavin cross-linking (CXL) is an increasingly used technique for the treatment of keratoconus, which aims at stiffening the corneal tissue. The increase in corneal rigidity gained with this treatment is assumed to result from the reaction of the photosensitizer (riboflavin) with UV light, which creates radicals that induce additional cross-links between collagen fibrils, probably interhelically, intrahelically, and intermicrofibrillary.[15,16] Strip extensiometry stress-strain experiments showed an increase in corneal rigidity immediately after and at several months post CXL in human,[2] porcine,[2] and rabbit[1] corneas. Also whole-globe inflation experiments showed an immediate increase in corneal rigidity in eyes in vitro after CXL.[11] The biomechanical response estimated from the previous methods may be affected by the corneal shape (geometry), thickness, hydration state (in vitro), and IOP (in vivo). In this study, we developed a new two-dimensional (2D) stress-strain system that allows maintaining the original stress distribution along the corneal flap, while guaranteeing that corneal hydration is equal for all samples. This allows an accurate comparison between individual flaps of a certain layer, as well as a precise analysis of the treatment effects on a few corneal layers. To prove its application, we evaluated the change in corneal rigidity following CXL treatment in rabbits.

Methods

Corneal flaps were mounted in a chamber connected to a pressure system that applied the force to stretch flaps of porcine and rabbit corneas. The flap deformation was monitored with a ray-tracing aberrometer (iTrace; Tracey Technologies Corp., Houston, TX). Rabbit

Investigative Ophthalmology & Visual Science, July 2012, Vol. 53, No. 8

flaps were treated with CXL in vivo. An analytical model was applied to estimate the tissue elasticity in non-treated corneas and after CXL.

Flap Holder

A custom flap holder (Fig. 1) was constructed for 2D stretching of a corneal flap. The holder consisted of two chambers separated by the flap: Chamber 1 was filled with riboflavin-dextran, permitting diffusion of the photosensitizer into the flap in both conditions (non-treated, one month after CXL). The chamber was connected to a pressure system in order to apply a normal surface load onto the flap. Chamber 2 was filled with Oxane 1300 Silicone Oil (Bausch & Lomb, Berlin, Germany) in order to preserve corneal hydration and because of its high refractive index (1.5). This chamber was left open to provide atmospheric pressure independent of pressure in Chamber 1. The dextran in the riboflavin solution in Chamber 1 regulated the flap's hydration, while the silicone oil prevented water evaporation. Under these conditions (ambient temperature, 25°C) flap hydration was maintained constant throughout treatment and measurements. The size of the opening between chambers where the flap was mounted had a diameter of 6 mm.

Pressure System

Pressure was modified infusing saline solution in Chamber 1 by an automatic pumping system, consisting of a syringe mounted on a custom built motorized stage. A pressure sensor (SSCM3175GA; Sensortechnics, Puchheim, Germany) was used in combination with a custom LabView routine to monitor the pressure difference between Chambers 1 and 2.

Eyes and Flap Preparation

In vitro experiments were performed in order to measure the elasticity of corneal flaps and to investigate the effect of changes in rigidity induced by CXL. Measurements were performed on fresh enucleated porcine eyes (non-treated), as well as on New Zealand rabbit eyes (non-treated and 1 month post in vivo CXL). Measurements in porcine eyes allowed establishing the technique, while measurements in rabbit eyes allowed evaluating the CXL treatment. Porcine eyes were obtained from a local slaughterhouse and used within 24 hours. Rabbits were obtained from a certified farm at the age of 3 months (~ 2 kg in weight).

After performing CXL treatment in the left eye, the rabbits were housed and cared for in animal facilities. A total of 13 porcine eyes and 8 rabbit eyes were tested. All animals were treated in accordance with the ARVO Statement for the Use of Animals in Ophthalmic and Vision Research, and had been approved by the institutional review board. In porcine eyes in vitro, first the epithelium was removed with a hockey epithelium removal knife (Katena Eye Instruments, Denville, New Jersey) and 20% Dextran (D8821; Sigma-Aldrich, Munich, Germany) solution was applied for 40 minutes. Then the IOP was adjusted to physiologic value (15 mm Hg). A flap was cut with a mechanical Carriazo-Pendular microkeratome (Schwind, Kleinostheim, Germany) and mounted on the custom holder. Ultrasonic pachymetry was performed for the intact eye and for the corneal bed after cutting the flap, in order to estimate the thickness of the removed flap. The extensiometry measurement was conducted in the untreated flap. Riboflavin-Dextran solution was constantly supplied by Chamber 1 from the moment when the flap was mounted within the system.

Rabbits were anaesthetized using 1 mL Ketamine hydrochloride 10% + 2 mL Xylazine 2%. CXL was performed following standard clinical conditions, first 30 minutes of riboflavin instillation, followed by 30 minutes 370 nm UV light exposure (Compact LED Area Light; Edmund Optics, Karlsruhe, Germany) of 3 mW/cm^2, while continuing riboflavin instillation every 3 minutes. Left eyes were treated and right eyes were left untreated for control. Rabbits were euthanized one month after treatment. Corneal flaps were excised immediately after euthanization, mounted on the flap holder, and the extensiometry measurement was done.

Rabbit eyes were examined with a confocal light microscope (HRT; Heidelberg Engineering, Heidelberg, Germany) at different times: before treatment, immediately after CXL, one day after CXL, and one month after CXL.

Extensiometry

Measurements were conducted for a series of pressures, for each flap, and condition. Initially, the pressure in Chamber 1 was set equal to pressure in Chamber 2 [1013 hectopascals (hPa)]. Then, one preconditioning cycle was performed up to the pressure of 35 mm Hg. Pressure was increased up to 30 mm Hg, and then decreased, in approximately 5 mm Hg steps. After preconditioning, ray tracing measurements were performed for two inflation-deflation cycles.

Figure 1. Flap mounting.

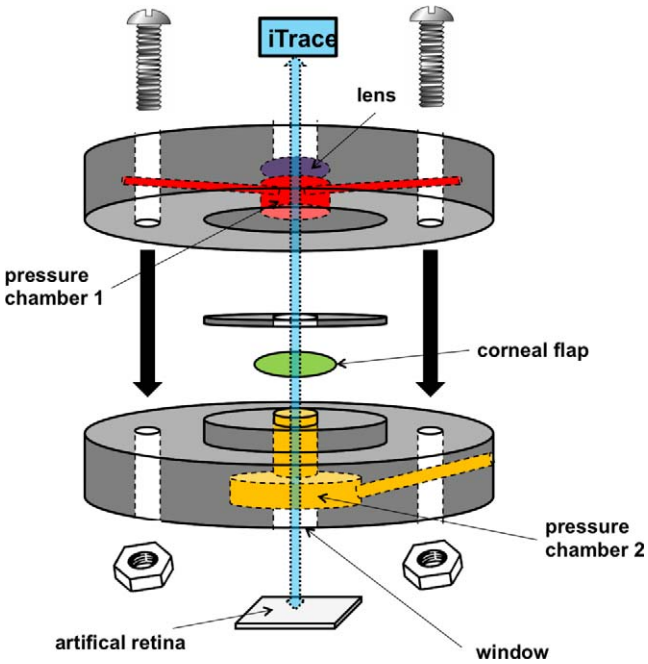

Figure 2. Measurement set up.

Ray Tracing Measurements

The geometry of the flap was assessed using ray tracing (iTrace; Tracey Technologies Corp.) at each pressure step. Flaps were mounted in the holder and the system was placed as an artificial eye in front of the iTrace for aberrometry measurements (Fig. 2). The measurement wavelength was 670 μm. Zernike coefficients (up to the seventh order) were obtained for a pupil diameter of 2.5 mm, and the low order terms (defocus and astigmatism) were used for analysis. Changes in the low order aberrations are related to changes in the curvature and astigmatism of the flap surface. Ray tracing measurements were obtained during two inflation cycles for each flap and condition, which in total took approximately 20 minutes. Measurements were performed in approximately 5 mm Hg pressure steps.

Data Analysis

The amount of defocus in the artificial eye is related to the stretching of the corneal flap. The higher the pressure in Chamber 1, the more curved the flap and the higher the change of the system's refractive power. Due to small deformations produced by the applied pressures, it can be assumed that the flap is deformed spherically. This approximation is further justified as we selected a central portion of the flap for measurement and analysis. Zernike coefficients Z_2^0 (defocus term) and Z_2^2 / Z_2^{-2} (astigmatism at 45°/90° terms) were analyzed. The defocus term was used to calculate the surface area of the flap as a function of pressure:

$$A_{flap}(p) = \int_0^{r_{flap}} Z_2^0(p) \times \sqrt{3} \times (2r^2 - 1)dr \quad (1)$$

where A_{flap} is the surface area, p is pressure in Chamber 1, and r the distance from the center of the optical axis.

Then, an analytical model was applied to obtain stress

$$\sigma = p_{chamber1} \times \left[(A_{flap})/(th \times 2r_{flap})\right] \quad (2)$$

and strain

$$\varepsilon = \sqrt{\Delta A_{flap}/A_{flap_0}} \quad (3)$$

from changes in the flap area, where *th* stands for thickness, σ for stress, and ε for strain. Stress is a measure of the amount of force acting on the cross-sectional area, and strain represents the relative expansion of the original flap area. The absolute pressure variation, and, hence, the applied force stretching the flap, was sufficiently small, so that elastic deformation only could be assumed. A linear fit was adjusted to the stress-strain relation in order to obtain the corresponding Young's modulus:

$$E = \Delta\sigma/\Delta\varepsilon \quad (4)$$

The Zernike terms Z_2^2 and Z_2^{-2} were used in order to calculate J_0 (horizontal astigmatism) and J_{45} (oblique astigmatism) following the power vector notation. The calculated astigmatism was analyzed as a function of pressure increase. Absolute differences in the astigmatism between CXL and non-treated flaps were investigated. A Student's *t*-test (two sample equal variance, two tailed) was applied to test the statistical differences in the flap shapes across conditions between non-treated and CXL.

Results

Flap Pachymetric and Microscopic Observations

Corneal flap thickness was 98 ± 21 μm in porcine and 96 ± 14 μm in rabbit corneas. After manual excision of the hinge, a 6-mm circular portion of the flap was mounted and measured. In compliance with other studies on confocal microscopy,[17] we observed highly reflective structures in the rabbit

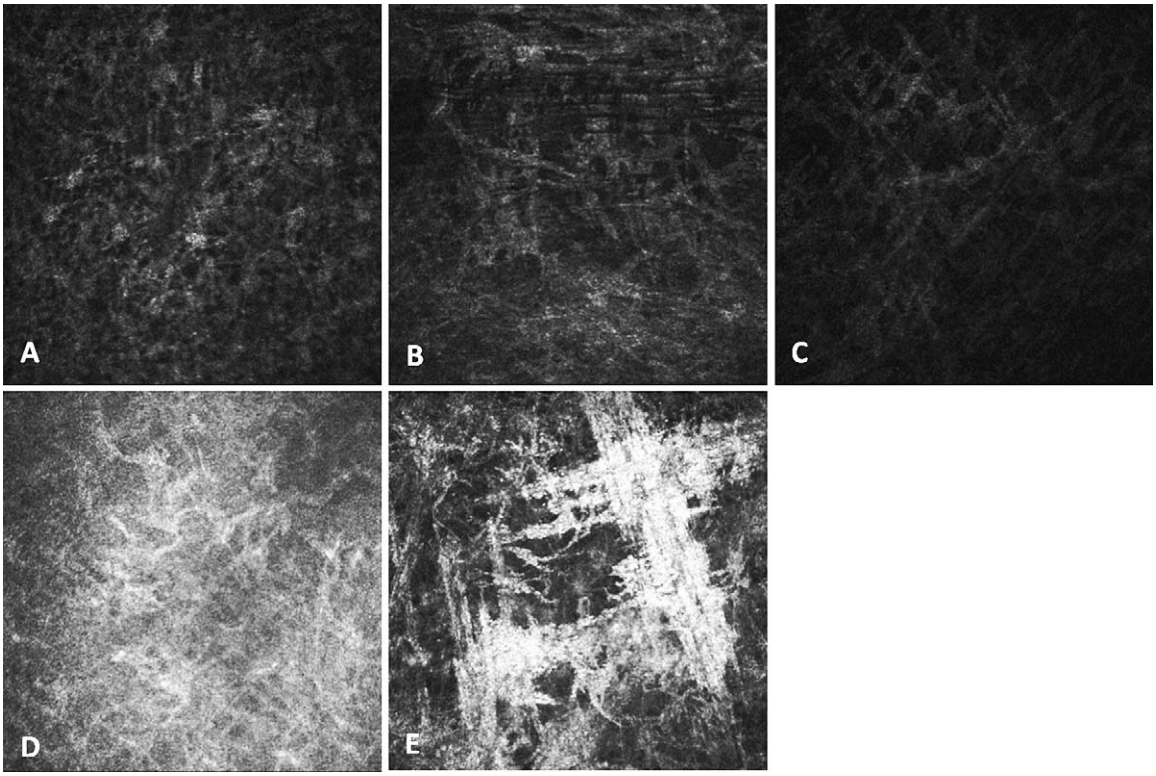

Figure 3. Confocal microscopy images comparing the midstroma (approximately 130 μm depth) in three conditions (rabbits): (**A**) virgin cornea, (**B**) riboflavin instillation, (**C**) immediately post CXL, (**D**) one day post CXL, and (**E**) one month post CXL.

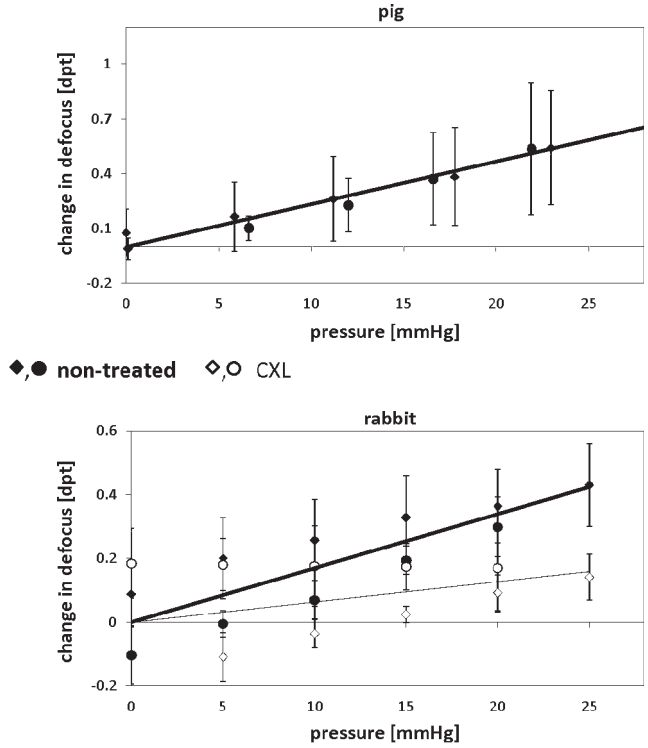

Figure 4. Changes in defocus as a function of pressure on the flap in (**A**) pig eyes and (**B**) rabbit eyes (non-treated versus CXL). *Diamonds* stand for pressure increase, and *circles* stand for pressure decrease. *Open symbols* represent cross-linked flaps and *closed symbols* non-treated flaps.

midstroma one month after CXL (Fig. 3). Interestingly, these structures could not be observed immediately after, or one day after, CXL.

Defocus Aberration

Figure 4 shows the change in the defocus term from the Zernike polynomial expansion as a function of pressure in Chamber 1 from porcine (Fig. 4A) and rabbit (Fig. 4B) flaps. Black symbols represent the control measurement, while white symbols stand for the cross-linked condition. Diamonds stand for increasing pressure and circles for decreasing pressure. Data of the three conditions are the average across 13 porcine corneas, 4 non-treated rabbit corneas, and 4 cross-linked rabbit corneas, respectively. SDs are plotted as error bars in Figure 4. Defocus increased linearly with increasing pressure in all conditions. Trend lines to the average of non-treated (bold) and CXL (thin) data show a positive slope. The lower the slope, the smaller the deformation and the stiffer the corneal flap. The slope in porcine flaps was 23.4×10^{-3} diopter (D)/mm Hg. In rabbit eyes the slope in the non-treated cornea (17.0×10^{-3} D/mm Hg) was significantly steeper ($P = 0.105$) than the cross-linked corneas (6.36×10^{-3} D/mm Hg), consistently with an increase in corneal rigidity after CXL. Variability across samples was 0.22 D in porcine flaps, 0.10 D in non-treated rabbit flaps, and 0.08 D in CXL rabbit flaps.

In certain conditions, the flap geometry did not recover its original state after pressure variation, showing a hysteresis. This can be seen by the differences in refractive power at the same pressure in the increasing and decreasing pressure sequences. Porcine corneas did not show this effect ($P = 0.338$). However, in rabbit corneas there was a significant shift in defocus (control: $P = 0.032$; CXL: $P = 0.007$) after the pressure increase/decrease cycle: 0.19 D in control flaps and 0.39 D in CXL flaps (at 0 mm Hg pressure). Actually, after CXL, the refraction hardly changed with pressure decrease, indicating a permanent plastic deformation. But the small sample size in rabbits might limit the impact of this finding.

Astigmatic Aberration

Mean astigmatism was modest, both in porcine flaps (0.55 D) and in rabbit flaps (0.74 D in non-treated, 0.34 D in CXL), and did not change significantly with pressure variation. In rabbit flaps, a small decrease was observed after CXL.

Young's Modulus

Young's moduli were calculated for the different conditions. The average Young's modulus in porcine flaps was 2.29 ± 1.63 MPa. The average Young's modulus of rabbit flaps was 1.98 ± 0.40 MPa and increased significantly ($P = 0.003$) one month after in vivo CXL (4.83 ± 1.32 MPa). Figure 5 shows the stress-strain diagram, calculated from average experimental data and equations for stress (equation 2) and strain (equation 3). Average data from the loading and unloading cycle were used

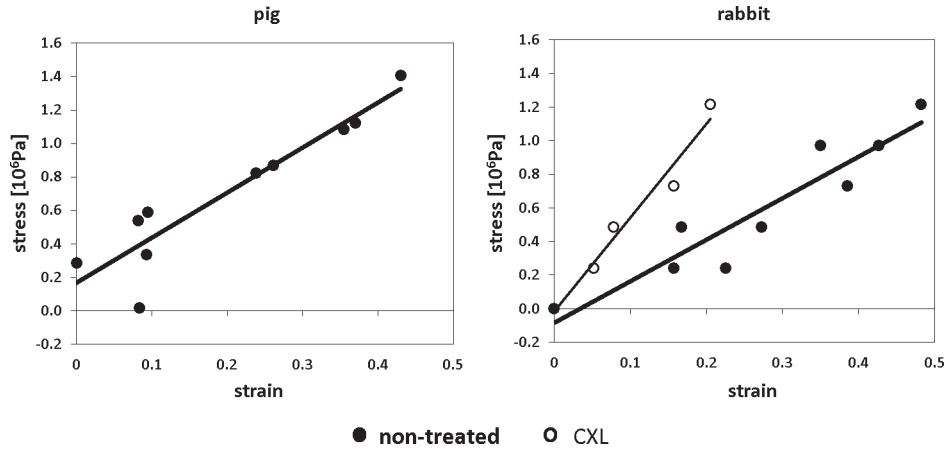

Figure 5. Stress strain diagrams in (**A**) pig eyes and (**B**) rabbit eyes (non-treated and CXL). The Young's modulus was estimated from the slope of the linear trend lines of the average data from the loading and unloading cycle. *Open circles* represent cross-linked flaps, and *closed circles* represent non-treated flaps.

to calculate the slopes, which represent Young's modulus according to equation 4.

Discussion

We present a 2D flap extensiometry technique, which allows measuring corneal elasticity parameters, minimizing the effects associated with corneal hydration, among others. This method has proved sensitive to detect differences across conditions, and could be used to investigate corneal biomechanical properties at different corneal depths. While in the current study we used a mechanical microkeratome (that limited the thickness accuracy to which the flaps could be cut), the use of a femtosecond laser would allow excising flaps of more resolved thickness and at different depth positions. The method could be used to assess biomechanical properties of different corneal layers (i.e., anterior and posterior stroma). This information is valuable to accurately represent the corneal biomechanical response by spatially resolved finite element models.

We evaluated the potential of the technique on corneal flaps from a porcine model, and investigated the biomechanical changes in the cornea 1 month after CXL in rabbit eyes. The estimated values of Young's moduli (porcine flap: 2.29 MPa; rabbit flap: 1.98 MPa) fall within the ranges reported in literature, although those vary over more than two orders of magnitude depending on the study.[1,2,5,6,8,13,18–20] As a reference, in vitro strip extensiometry experiments estimated a Young's modulus of 11.1 MPa for rabbit corneas and 1.5 MPa for porcine corneas.[1,2] An in vitro button inflation study reported a Young's modulus of 2.87–19.5 MPa for the human cornea,[8] and a recent study using in vitro whole globe inflation in porcine eyes reported a Young's modulus of 1.11 MPa (Kling S, et al. *IOVS* 2010;51:ARVO E-Abstract 4628). Ultrasound measurements on in vitro human corneas provided a value of 5.3 MPa,[21] and an in vivo approach based on the deformation with applanation tonometry 0.29 MPa in humans.[22] The large differences across reports of Young's modulus likely arise from the different working principles of the techniques, and the hydration condition in which corneal tissue is measured. The Young's modulus in porcine eyes measured in this study agree well with extensiometry reports by Wollensak et al.[2] and inflation models by Kling et al.[11] It is likely that the higher elasticity values found for the flap compared with the Young's modulus of the entire cornea arise from the fact that only the most anterior layer of the corneal stroma was used in the flap study, as the anterior stroma has been reported to be stiffer than the posterior cornea.[23]

The proposed 2D flap extensiometry technique reduces the variability by controlling the flap thickness, avoids a major role of hydration, and allows a better spatially resolved analysis. The technique, therefore, combines several advantages from previous methods. First, it guarantees a very similar distribution of the acting force (pressure) to the in vivo condition, similar to button or whole globe inflation. As flaps are cut in a predefined thickness, the variation across specimens decreases. Second, the rigid circular fixation of the flap allows an accurate analysis of the corneal expansion, similarly to strip extensiometry, but preserving a more realistic geometry and the actual orientation of the collagen fibers.

The increase in corneal stiffness that we found after CXL in rabbits (× 2.43) is consistent with the literature. Previous studies reported an increase of corneal stiffness by a factor of 1.58–1.8 (in pigs), by 4.5 (in humans), and by 1.6 (in rabbits).[11,1,2] Again, the slightly higher factor can be explained because the flaps were cut on the anterior stroma. A study of the long term effects of CXL in rabbits (measured before and immediately after, and 3 and 8 months after CXL) showed a high stability in the post CXL corneal stiffness (a constant pre/post Young modulus ratio over time, by 1.6).[1]

Although there are studies reporting an immediate effect of CXL,[2,11] we suggest that apart from this, processes happening at the tissue level (e.g., wound healing) could contribute to the increase in corneal rigidity after CXL, as structural changes (highly reflective structures; Fig. 3) were observed to appear simultaneously with an increase in corneal rigidity.

In a previous study in porcine eyes in vitro,[11] we showed stronger stiffening effects of CXL in the horizontal than in the vertical direction. In the current study, a slight reduction of corneal astigmatism with CXL was observed in rabbits, which has also been reported clinically in patients.[22]

As a side effect, we observed that porcine corneal flaps did not show differences in the variation of the geometry with increased/decreased pressure, whereas in rabbit flaps a hysteresis was apparent.

The current study on cornel flaps suggests that the spatially resolved analysis (in this case in thin corneal layers) of the processes occurring in CXL may give insights into the understanding of its mechanisms. The use of new techniques (such as second harmonic microscopy[24]) that allow visualizing collagen at its structural level in combination with the presented 2D flap approach may lead to interesting advances in the future.

Acknowledgments

We thank Creta Farm S.A. for providing us with enucleated porcine eyes, G. Kontadakis, N. Kariotakis, and A. Papadiamantis for technical assistance.

References

1. Wollensak G, Iomdina E. Long-term biomechanical properties of rabbit cornea after photodynamic collagen crosslinking, *Acta Ophthalmol*. 2009;87;48–51.
2. Wollensak G, Spoerl E, Seiler T. Stress-strain measurements of human and porcine corneas after riboflavin-ultraviolet-A-induced cross-linking. *J Cataract Refract Surg*. 2003;29:1780–1785.
3. Elsheikh A, Kassem W, Jones SW. Strain-rate sensitivity of porcine and ovine corneas. *Acta Bioeng Biomech*. 2011;13:25–36.
4. Elsheikh A, Anderson K. Comparative study of corneal strip extensometry and inflation tests. *J R Soc Interface*. 2005;2:177–185.
5. Boyce BL, Grazier JM, Jones RE, Nguyen TD. Full-field deformation of bovine cornea under constrained inflation conditions. *Biomaterials*. 2008;29:3896–3904.
6. Knox Cartwright NE, Tyrer JR, Marshall J. Age-related differences in the elasticity of human cornea. *Invest Ophthalmol Vis Sci*. 2011;52:4324–4329.
7. Jue B, Maurice DM. The mechanical properties of the rabbit and human cornea. *J Biomech*. 1986;19:847–853.
8. Hjortdal JO. Regional elastic performance of the human cornea. *J Biomech*. 1996;29:931–942.
9. Litwiller DV, Lee SJ, Kolipaka A, et al. MR elastography of the ex vivo bovine globe. *J Magn Reson Imaging*. 2010;32:44–51.
10. Pierscionek BK, Asejczyk-Widlicka M, Schachar RA. The effect of changing IOP on the corneal and sclera curvatures in the fresh porcine eye. *Br J Ophthalmol*. 2007;91:801–803.
11. Kling S, Remón L, Pérez-Escudero A, Merayo-Lloves J, Marcos S. Corneal biomechanical changes after collagen cross-linking

from porcine eye inflation experiments. *Invest Ophthalmol Vis Sci*. 2010;51:3961–3968.

12. Dorronsoro C, Pascual D, Pérez-Merino P, Kling S, Marcos S. Dynamic OCT measurement of corneal deformation by an air puff in normal and cross-linked corneas. *Biomed Opt Exp*. 2012;3:473–487.
13. Hamilton KE, Pye DC. Young's modulus in normal corneas and the effect on applanation tonometry. *Optom Vis Sci*. 2008;85: 445–450.
14. Hjortdal JO. Extensibility of the normo hydrated human cornea. *Acta Opthalmol Scand*. 1995;73:12–17.
15. Abad JC, Panesso JL. Corneal collagen cross-linking induced by UVA and riboflavin. *Techniques in Ophthalmology*. 2008; 6:8–12.
16. Wollensak G, Wilsch M, Spoerl E, Seiler T. Collagen fiber diameter in the rabbit cornea after collagen crosslinking by riboflavin/UVA. *Cornea*. 2004;23:503–507.
17. Guthoff RF, Zhivov A, Stach O. In vivo confocal microscopy, an inner vision of the cornea—a major review. *Clin Experiment Ophthalmol*. 2009;37:100–117.
18. Kohlhaas M, Spoerl E, Schilde G, Unger G, Wittig C, Pillunat LE. Biomechanical evidence of the distribution of cross-links in corneas treated with riboflavin and ultraviolet A light. *J Cataract Refract Surg*. 2006;32:279–283.
19. Hjortdal JO, Jensen PK. In vitro measurement of corneal strain, thickness and curvature using digital image processing. *Acta Opthalmol Scand*. 1995;73:5–11.
20. Wang H, Prendiville PL, McDonnell PJ, Chang WV. An ultrasonic technique for the measurement of the elastic moduli of human cornea. *J Biomech*. 1996;29:1633–1636.
21. Sedaghat M, Naderi M, Zarei-Ghanavati M. Biomechanical parameters of the cornea after collagen crosslinking measured by waveform analysis. *J Cataract Refract Surg*. 2010;36:1728–1731.
22. Raiskup-Wolf F, Hoyer A, Spoerl E, Pillunat LE. Collagen crosslinking with riboflavin and ultraviolet-A light in keratoconus: long-term results. *J Cataract Refract Surg*. 2008;34: 796–801.
23. Hennighausen H, Feldman ST, Bille JF, McCulloch AD. Anterior-posterior strain variation in normally hydrated and swollen rabbit cornea. *Invest Opthalmol Vis Sci*. 1998;39:253–262.
24. Bueno JM, Gualda EJ, Giakoumaki A, Pérez-Merino P, Marcos S, Artal P. Multiphoton microscopy of ex vivo corneas after collagen cross-linking. *Invest Opthalmol Vis Sci*. 2011;52: 5325–5331.